J|A|C|S
COMMUNICATIONS

Published on Web 09/30/2004

Mechanism of the Stoddart−Heath Bistable Rotaxane Molecular Switch

Wei-Qiao Deng, Richard P. Muller, and William A. Goddard III*

Materials and Process Simulation Center, California Institute of Technology, Pasadena, California 91125

Received June 3, 2003; E-mail: wag@wag.caltech.edu

Molecular-scale electronics is developing rapidly[1] because of advances in the synthesis of suitably tailored organic structures, bringing us closer to the ultimate miniaturization of nanoelectronic devices.[2,3] In a recent success, the Stoddart and Heath groups designed rotaxanes (which have a ring molecule encircling the dumbbell-shaped molecule in Scheme 1) that function as a programmable electronic switch.[4−9] There are two likely sites for the ring molecule to localize: the tetrathiafulvalene group (TTF) in the left half and the 1,5-dioxynaphthalene group (DNP) in the right half. The experiments showed conclusive evidence of two distinct states (one with a resistance 10−100 times that of the other) and that the system could be switched from one state to the other by applying a sharp address voltage or applying a suitable oxidant or reductant. It is assumed that the switching behavior arises from the difference in conductivity between the two states. However, the atomistic-level mechanism of the switch is still unknown.

To provide the molecular-level understanding necessary to design and optimize such nanoelectronic devices, we initiated theoretical studies of the switching mechanism for the bistable [2]rotaxane shown in Scheme 1, which is based on formula I in Figure 3 of ref 8, but without the stoppers at each end. The detailed simulation procedures are given in the Supportive Information.

The calculation of electric conductivity at the atomic level is now well established.[10−14] The $I-V$ curves calculated by combination of quantum mechanics[15−19] and Green's function theory[12−14] for the two states of the rotaxane molecule are shown in Figure 1. Current flow through the state with the ring on the DNP group (R-DNP) increases almost linearly to 1.5 nA from 0 to 0.25 V bias and reach its maximum of 1.8 nA after 0.3 V. However, current through the state with the ring molecule on the TTF group (R-TTF) increases only to 0.05 nA at range from 0 to 0.5 V, shown in Figure 1b. The calculation results show large different conductivities between the R-DNP and R-TTF states. For applied bias from 0.01 to 0.2 V, the calculated ON/OFF ratio increases from 37 to 58 and decreases to 39 from 0.2 to 0.5 V applied bias. This ON/OFF ratio is comparable to experimental values[7] of 10−100. This suggests that the simulation has captured the essence of the experimental system. In particular, we find that the switch is OFF when the ring is on the TTF group (R-TTF) and ON when the ring is on the DNP group (R-DNP). Exactly this same assignment was previously proposed.[4,8]

Next we examine the orbital basis for the switching behavior. The frontier MOs, including highest occupied molecular orbital (HOMO), lowest occupied MO (LUMO), and nearby orbitals of the R-DNP and R-TTF states, are shown in Figure 2, respectively. More MOs can be found in the Supporting Information. These MOs contain contributions from four groups of atoms: Au electrode atoms at each end, the TTF group, the DNP group, and the ring group. We find two states with distinct $I-V$ differences:

• R-DNP state (ON): The HOMO is delocalized over the TTF and ring groups. The LUMO and LUMO+1 (0.1 eV above the LUMO) are delocalized over the TTF and ring-DNP groups. HOMO−1 is localized near the upper Au electrode.

• R-TTF state (OFF): HOMO−2 is localized at DNP; LUMO and LUMO+1 are localized at the TTF. HOMO−1 and HOMO are mostly localized at the electrodes.

Since the transmission function determines the electrical properties of the system, we establish a correspondence between the molecular MOs with the peaks in the transmission function. The correlation is shown in Figure 3. The frontier MOs exactly match the peaks in the transmission function (except for the MOs localized on Au, which do not contribute to conductivity). For the R-DNP/ON state, HOMO, LUMO, and LUMO+1 correspond to the three

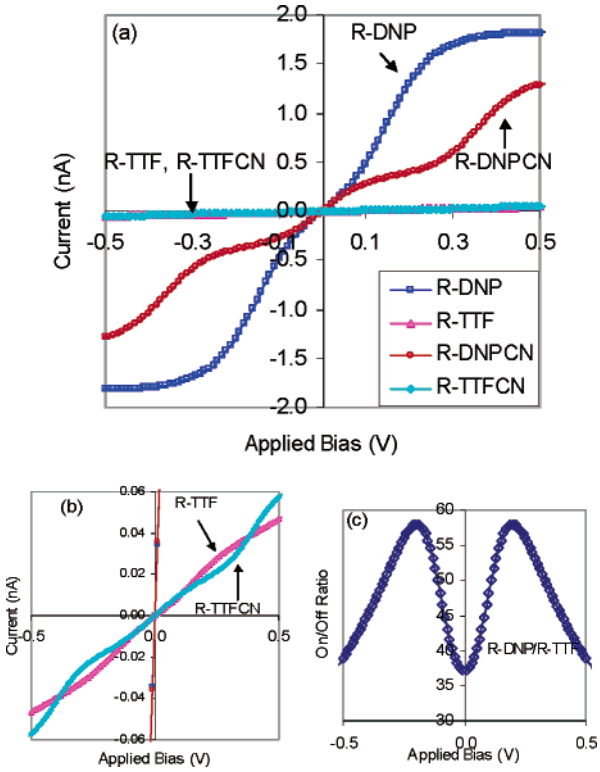

Figure 1. $I-V$ curve of Au−rotaxane−Au switch. (a) The four $I-V$ curves correspond to ring on DNP (R-DNP), on TTF (R-TTF), and for the modified version of the rotaxane bearing a CN group substituted on the DNP unit, R-DNPCN, and R-TTFCN states. (b) Small-scale $I-V$ curve of R-TTF and R-TTFCN. (c). The voltage-dependent ON/OFF ratio.

Scheme 1. Rotaxane Molecule Used in Our Simulation (Each Au Electrode Includes Three Au Atoms)

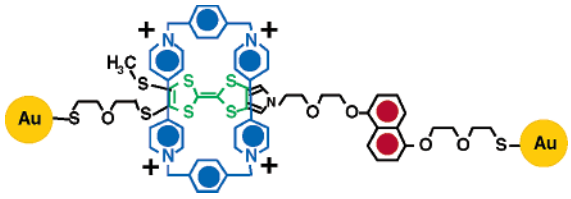

10.1021/ja036498x CCC: $27.50

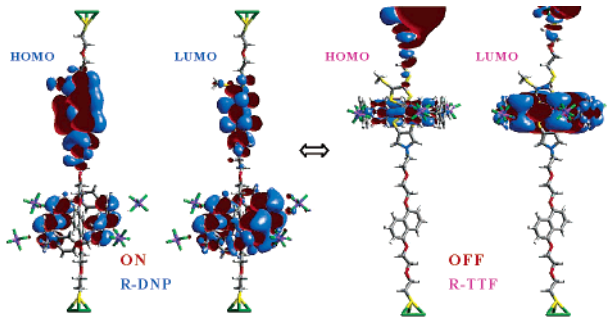

Figure 2. MOs of Au−rotaxane−Au switch. Green represents Au atoms, yellow is S, gray is C, red is oxygen, and white is hydrogen. The ring is $CBPQT^{4+}$, with 4 PF_6^- units around. The TTF and DNP units are located at the top and bottom halves of the dumbbell, respectively. The total is 186 atoms.

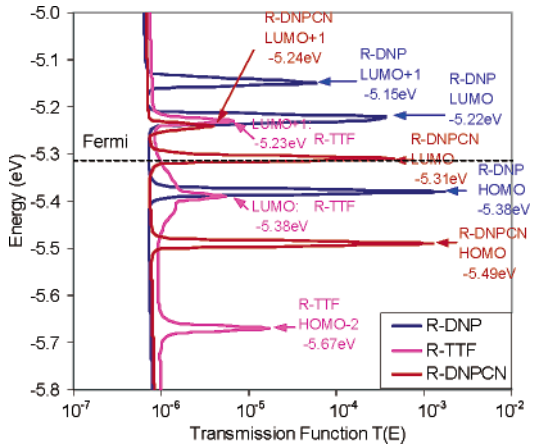

Figure 3. Transmission function of rotaxane components. Blue curve is for R-DNP, pink curve is for R-TTF, and red curve is for R-DNPCN. The dashed line is the Fermi energy of Au electrodes, −5.31 eV.

peaks in Figure 3 where HOMO contributes the highest peak (blue) because it is the most delocalized MO. For the R-TTF/OFF state, the HOMO−2, LUMO, and LUMO+1 lead to three peaks (pink). These MOs are localized, leading to transmission peaks 10−1000 times smaller than the peaks of the ON state. Thus, we conclude that the characteristics of the MOs around the Fermi energy determine the electrical conductivities of the Au−rotaxane−Au system.

With a plausible mechanism for understanding the switch in the rotaxane system, we can now use this mechanism to design improved devices. For example, chemical groups could be attached to the rotaxane molecule so as to shift the frontier orbitals to make them more localized for the OFF state and/or more delocalized for the ON state. Therefore, to optimize the rotaxane switch, we are considering changes such as those in Scheme 2, where each component of the switch can be functionalized separately. Which group best optimizes the switch depends on which frontier orbital is tuned. To illustrate the procedure, we added a CN group, an electron acceptor, on the DNP site to shift the characteristic of that orbital and change the distribution of the frontier orbitals. The red curve in Figure 3 shows the transmission with CN modification. The CN addition makes LUMO+1 more localized, leading to a smaller transmission. This suggests that we should add the CN instead to the TTF region.

A second reversible molecular switch consisting of a metal−molecule−metal sandwich has been reported recently. However, the mechanism in this switch has been demonstrated to result from the growth and dissolution of metallic nanoparticles,[20] quite different from the Heath−Stoddart system we consider here. This molecular switch may be similar to Yang's bistable contact/organic/metal nanoparticle/organic/contact device.[21]

Scheme 2. Strategy for the Modifications of the Rotaxane Switch

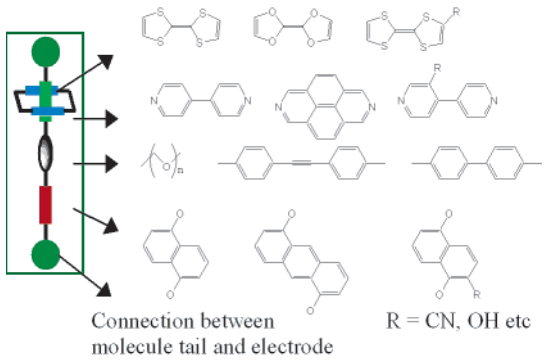

Summarizing, we used quantum mechanics to simulate the performance of the Stoddart−Heath rotaxane switch. We find two states with a ∼40−60 difference in conductance and determined that R-DNP is the ON state while R-TTF is OFF, supporting the mechanism proposed by Stoddart.[8,9] The change in the delocalization of the MOs affected by the ring movement plays a key role in the switching mechanism. Using this mechanism, we can now estimate how changes in the chemical components will change switch performance, providing a design principle for optimization.

Acknowledgment. We thank Fraser Stoddart, James Heath, Supriyo Datta, Xin Xu, and Amar Flood for helpful discussions. This research was supported by NSF-NIRT and MARCO-FENA.

Supporting Information Available: Computational methods and detailed results. This material is available free of charge via the Internet at http://pubs.acs.org.

References

(1) Tseng, G. Y.; Ellenbogen, J. C. *Science* **2001**, *294*, 1293.
(2) Feynmann, R. P. In *Miniaturization*; Gilbert, H. D., Ed.; Reinhold: New York, 1961; p 282.
(3) Aviram, A.; Ratner, M. A. *Chem. Phys. Lett.* **1974**, *29*, 277.
(4) Collier, C. P.; Mattersteig, G.; Wong, E. W.; Luo, Y.; Beverly, K.; Sampaio, J.; Raymo, F. M.; Stoddart, J. F.; Heath, J. R. *Science* **2000**, *289*, 1172.
(5) Wong, E. W.; Collier, C. P.; Behloradsky, M.; Raymo, F. M.; Stoddart, J. F.; Heath, J. R. *J. Am. Chem. Soc.* **2000**, *122*, 5831.
(6) Collier, C. P.; Wong, E. W.; Belohradsky, M.; Raymo, F. M.; Stoddart, J. F.; Kuekes, P. J.; Williams, R. S.; Heath, J. R. *Science* **1999**, *285*, 391.
(7) Collier, C. P.; Jeppesen, J. O.; Luo, Y.; Perkins, J.; Wong, E. W.; Heath, J. R.; Stoddart, J. F. *J. Am. Chem. Soc.* **2001**, *123*, 12632.
(8) Luo, Y.; Collier, C. P.; Jeppesen, J. O.; Nielsen, K. A.; Delonno, E.; et. al *ChemPhysChem* **2002**, *3*, 519.
(9) Pease, A. R.; Jeppesen, J. O.; Stoddart, J. F.; Luo, Y.; Collier C. P.; Heath, J. R. *Acc. Chem. Res.* **2001**, *34*, 433.
(10) Lang, N. D. *Phys. Rev. B* **1995**, *52*, 5335. Lang, N. D. *Phys. Rev. Lett.* **1997**, *79*, 1357.
(11) Datta, S. *Electronic Transport in Mesoscopic Physics*; Oxford University Press: Oxford, 1997.
(12) Yaliraki, S. N.; Roitberg, A. E.; Gonzalez, C.; Mujica, V.; Ratner, M. A. *J. Chem. Phys.* **1999**, *111*, 6997.
(13) Xue, Y. Q.; Datta S.; Ratner, M. A. *J. Chem. Phys.* **2001**, *115*, 4292.
(14) Seminario, J. M.; Zacarias, A. G.; Derosa, P. A. *J. Phys. Chem. A* **2001**, *105*, 791.
(15) Mayo, S. L.; Olafson, B. D.; Goddard, W. A. *J. Chem. Phys.* **1990**, *94*, 8897.
(16) Mopac2000 package, Schrodinger Inc., Portland, OR.
(17) Hay, P. J.; Wadt, W. R. *J. Chem. Phys.* **1985**, *82*, 299.
(18) Jaguar 4.0, Schrodinger Inc., Portland, OR.
(19) Papaconstantopoulos, D. A. *Handbook of the band structure of Elemental Solids*; Plenum Press: New York, 1986.
(20) Heath, J. R.; Stoddart, J. F.; Williams, R. S. *Science* **2004**, *303*, 1136.
(21) Wu, J. H.; Ma, L. P.; Yang, Y. *Phys. Rev.* **2004**, *69*, 115321.

JA036498X